Gen Relativ Gravit (2011) 43:819–832
DOI 10.1007/s10714-010-1103-4

RESEARCH ARTICLE

Combined constraints on modified Chaplygin gas model from cosmological observed data: Markov Chain Monte Carlo approach

Jianbo Lu · Lixin Xu · Yabo Wu · Molin Liu

Received: 15 July 2010 / Accepted: 20 September 2010 / Published online: 15 October 2010

Abstract We use the Markov Chain Monte Carlo method to investigate a global constraints on the modified Chaplygin gas (MCG) model as the unification of dark matter and dark energy from the latest observational data: the Union2 dataset of type supernovae Ia (SNIa), the observational Hubble data (OHD), the cluster X-ray gas mass fraction, the baryon acoustic oscillation (BAO), and the cosmic microwave background (CMB) data. In a flat universe, the constraint results for MCG model are, $\Omega_b h^2 = 0.02263^{+0.00184}_{-0.00162}(1\sigma)^{+0.00213}_{-0.00195}(2\sigma)$, $B_s = 0.7788^{+0.0736}_{-0.0723}(1\sigma)^{+0.0918}_{-0.0904}(2\sigma)$, $\alpha = 0.1079^{+0.3397}_{-0.2539}(1\sigma)^{+0.4678}_{-0.2911}(2\sigma)$, $B = 0.00189^{+0.00583}_{-0.00756}(1\sigma)^{+0.00660}_{-0.00915}(2\sigma)$, and $H_0 = 70.711^{+4.188}_{-3.142}(1\sigma)^{+5.281}_{-4.149}(2\sigma)$.

Keywords Modified Chaplygin gas (MCG) · Unification of dark matter and dark energy

J. Lu · Y. Wu
Department of Physics, Liaoning Normal University, Dalian 116029, People's Republic of China
e-mail: lvjianbo819@163.com

Y. Wu
e-mail: ybwu61@163.com

L. Xu (✉)
School of Physics and Optoelectronic Technology, Dalian University of Technology, Dalian 116024, People's Republic of China
e-mail: lxxu@dlut.edu.cn

M. Liu
College of Physics and Electronic Engineering, Xinyang Normal University, Xinyang 464000, People's Republic of China

1 Introduction

Recently, mounting cosmic observations suggest that the expansion of present universe is speeding up rather than slowing down [1–4]. And it indicates that baryon matter component is about 5% of the total energy density, and about 95% of the energy density in the universe is invisible, including dark matter (DM) and dark energy (DE). In addition, it is shown that DE takes up about two-thirds of the total energy density from cosmic observations. In theory many kinds of DE models [5–15] have already been constructed to explore the DE properties.

Chaplygin gas (CG) and its generalized model have been widely studied for interpreting the accelerating universe [16–20]. The CG model can be obtained from the string Nambu–Goto action in the light cone coordinate [21,22]. For generalized Chaplygin gas (GCG), it emerges as a effective fluid of a generalized d-brane in a $(d+1, 1)$ space time, and its action can be written as a generalized Born–Infeld form [23]. Considering that the application of string theory in principle is in very high energy when the quantum effects is important in early universe [21,22], the quantum cosmological studis of the CG and the GCG has been well investigated in Ref. [21,22] and [24]. In addition, one knows that the most attractive property for these models is, two unknown dark sections in universe—dark energy and dark matter can be unified by using an exotic equation of state. It is worthwhile to study the unified models of dark sections for other generalization of CG.

A simple and popular generalization relative to the GCG model is that it is extended to a form by adding a barotropic term, referred to as the modified Chaplygin gas (MCG) [25,26]. The correspondences between the MCG and the ordinary scalar field [25,26], the tachyon theory [25–29], and the holographic dark energy density [30,31] of the universe have been studied. In principle, MCG represents the evolution of the universe starting from the radiation era to the era dominated by the cosmological constant [32–35]. In addition, MCG is also applied to inflation theory [36–39]. For the more discussion on MCG model, please see Refs. [40–48]. In this paper, we use the Markov Chain Monte Carlo (MCMC) technique to constrain this more general unified candidate, MCG. The used observational data include, the Union2 data of type Ia supernovae (SNIa) [49,50], the observational Hubble data (OHD) [51], the cluster X-ray gas mass fraction [52], the measurement results of baryon acoustic oscillation (BAO) from Sloan Digital Sky Survey (SDSS) and Two Degree Field Galaxy Redshift Survey (2dFGRS) [53,54], and the current cosmic microwave background (CMB) data from seven-year WMAP [55].

2 Modified Chaplygin gas model

We briefly introduce the GCG model as the unification of dark matter and dark energy at first. The energy density ρ and pressure p in this model are related by the equation of state (EOS)

$$p_{GCG} = -\frac{A}{\rho_{GCG}^{\alpha}}, \tag{1}$$

where A and α are parameters in the model. When $\alpha = 1$, it is reduced to the CG scenario. Using Eq. (1) one has a solution of energy density for the GCG fluid

$$\rho_{GCG} = \rho_{0GCG}\left[A_s + \frac{1 - A_s}{a^{3(1+\alpha)}}\right]^{\frac{1}{1+\alpha}}, \tag{2}$$

where $\mathrm{A}_s = \frac{A}{\rho_{0GCG}^{1+\alpha}}$. From Eq. (2) one can see that the GCG fluid behaves as a dust-like matter at early time and as a dynamical cosmological constant at late epoch [56–63], then the GCG can be interpreted as an entangled mixture of dark matter and dark energy. The dual role of the GCG fluid is at the heart of the interesting property of this model.

For MCG model, from phenomenological view point it is interesting and can be motivated by the brane world interpretation [64]. It is characterized by a more general EOS,

$$p_{MCG} = B\rho_{MCG} - \frac{A}{\rho_{MCG}^{\alpha}}, \tag{3}$$

which looks like that of two fluids, one obeying a perfect EOS $p = B\rho$ and the other being the GCG [25,26]. Where A, B, and α are parameters in the model, ρ_{MCG} and p_{MCG} are energy density and pressure of the MCG fluid. From Eq. (3), it is easy to see that the EOS of MCG reduces to the GCG scenario if $B = 0$, and reduces to the perfect fluid if $A = 0$. In addition, with $B = 0$ and $\alpha = 0$ it reduces to ΛCDM model. In the space–time geometry described by the non-flat Friedmann–Robertson–Walker (FRW) metric

$$ds^2 = -dt^2 + a^2(t)\left[\frac{dr^2}{1 - kr^2} + r^2(d\theta^2 + \sin^2\theta d\phi^2)\right], \tag{4}$$

the EOS (3) leads, after inserted into the relativistic energy conservation equation, to an energy density of MCG evolving as

$$\rho_{MCG} = \rho_{0MCG}\left[B_s + \frac{1 - B_s}{a^{3(1+B)(1+\alpha)}}\right]^{\frac{1}{1+\alpha}}, \tag{5}$$

for $B \neq -1$, where $\mathrm{B}_s = \frac{A}{(1+B)\rho_{0MCG}^{1+\alpha}}$, a is the scale factor of universe which is related to the redshift by, $a = \frac{1}{1+z}$. Considering that MCG fluid plays the role of a mixture of dark matter and dark energy, and assuming that the universe is filled with three components: the MCG, the baryon matter, and the radiation component, one can express the dimensionless Hubble parameter E as

$$\begin{aligned} E &= \frac{H}{H_0} \\ &= \sqrt{(1 - \Omega_b - \Omega_r - \Omega_k)[B_s + (1 - B_s)a^{-3(1+B)(1+\alpha)}]^{\frac{1}{1+\alpha}} + \Omega_b a^{-3} + \Omega_r a^{-4} + \Omega_k a^{-2}}, \end{aligned} \tag{6}$$

where H is the Hubble parameter, with its current value $H_0 = 100h$ km s^{-1} Mpc^{-1}, Ω_b, Ω_r, and Ω_k denote the dimensionless baryon matter, radiation, and curvature density, respectively.

3 Constraint result and conclusion

Next we apply the current observed data to constrain the MCG model. The constraint method and the used data: Union2 SNIa, OHD, CBF, BAO, and CMB data are presented in Appendix A. In our calculations the total likelihood function is written as $L \propto e^{-\chi^2/2}$, with the total χ^2 equaling

$$\chi^2 = \widetilde{\chi}^2_{SNIa} + \chi^2_{OHD} + \chi^2_{CBF} + \chi^2_{BAO} + \chi^2_{CMB}, \tag{7}$$

where the separate likelihoods of SNIa, OHD, CBF, BAO and CMB are given by Eqs. (A9), (A12), (A16), (A24) and (A28). From the expressions of χ^2_{CBF}, χ^2_{BAO} and χ^2_{CMB}, one can see that they are related with the matter density Ω_m. For MCG model, since it is considered as the unification of dark matter and dark energy, we do not have dark matter in this model. So, the matter density is not explicitly included in the background Eq. (6). According the Eq. (6), by considering the universe is dominated by the matter component at early time ($a \ll 1$), i.e., relative to the dark matter density the dark energy density is neglectable, one can get an effective expression of the current matter density, $\Omega_m = \Omega_b + (1 - \Omega_b - \Omega_r - \Omega_k)(1 - A_s)^{\frac{1}{1+\alpha}}$. This expression of Ω_m, is an estimate of the "matter" component of the MCG fluid with the baryon density. Thus, in the CBF, BAO and CMB constraints, we take this expression of Ω_m.

Next, we perform a global fitting on determining the MCG model parameters using the Markov Chain Monte Carlo (MCMC) approach. In our joint analysis, the MCMC code is based on the publicly available **CosmoMC** package [65] and the **modified CosmoMC** package [52,66,67]. The latter package is about the constraint code of X-ray cluster gas mass fraction, with including additional 7 free parameters $(K, \eta, \gamma, b_0, \alpha_b, s_0, \alpha_s)$. In these packages, they have been modified to include the new model parameters B_s, α and B. In the calculation the baryon matter density is taken to be varied with a tophat prior: $\Omega_b h^2 \in [0.005, 0.1]$. In addition, for the MCMC calculation on the MCG model, we run 8 independent chains, and to get the converged results we test the convergence of the chains by typically getting $R - 1$ to be less than 0.03.

In Fig. 1, we show a one-dimensional probability distribution of each parameter and two-dimensional plots for parameters between each other in the flat MCG model. According to the figure, the constraint results on the best fit values of parameters with 1σ and 2σ confidence levels are listed in Table 1. In Ref. [34,35] it is shown that for the constraint on MCG model parameters obtained from the sound speed, $0 < c_s^2 < c^2$, the parameters are restricted to $0 < (B + 1)(\alpha + 1) < 2$. According to this constraint on MCG model parameters one can see that the MCG fluid has a well sound speed. Considering Ref. [42], where the model parameter B is constrained by using the location of the peak of the CMB spectrum, $-0.35 \lesssim B \lesssim 0.025$, it is easy to see that our result is more stringent. In addition, considering Ref. [68], where the values of

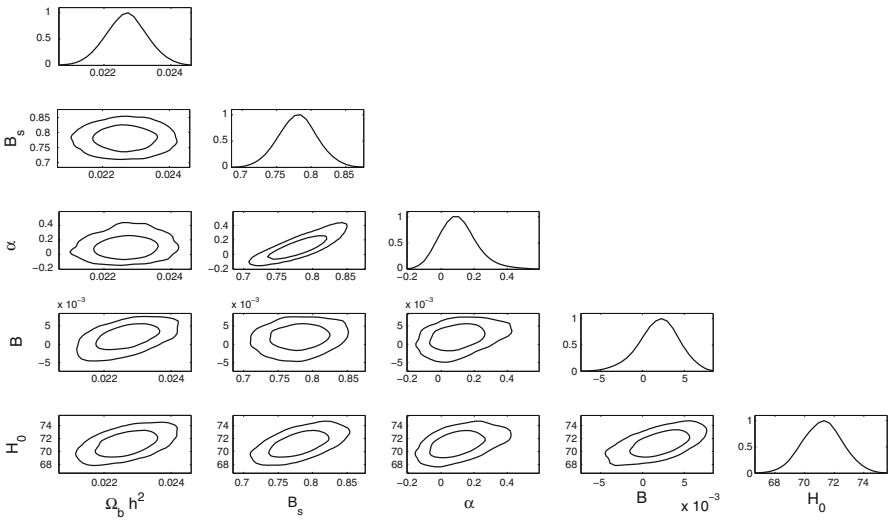

Fig. 1 The 2-D contours with $1\sigma, 2\sigma$ confidence levels and 1-D marginalized distribution of $\Omega_b h^2$, B_s, α, B, and H_0 in the flat MCG model

Table 1 The data fitting results of the MCG model parameters with 1σ and 2σ confidence levels

Parameters	Best fit values
$\Omega_b h^2$	$0.02263^{+0.00184+0.00213}_{-0.00162-0.00195}$
B_s	$0.7788^{+0.0736+0.0918}_{-0.0723-0.0904}$
α	$0.1079^{+0.3397+0.4678}_{-0.2539-0.2911}$
B	$0.00189^{+0.00583+0.00660}_{-0.00756-0.00915}$
H_0	$70.711^{+4.188+5.281}_{-3.142-4.149}$
$\chi^2_{min}(\chi^2_{min}/dof)$	596.147 (0.9709)

model parameters are analyzed against the matter power spectrum observational data, it is obtained that a very stringent constraint exists on B, which is consistent with our result, i.e., it seems that the MCG model is viable only for very special cases, and it tends to reduce to the GCG scenario.

In addition, we consider a more general non-flat background geometry. For using above combined observational data to constrain the MCG model, since the space curvature Ω_k is near to zero, the constraint results of the model parameters obtained from the non-flat universe are similar to the cases of the flat universe. For simplicity, we do not list the constraint results for this case. With replacing the Union2 SNIa data[1] with the 397 Constitution data[2] [69] in the above

[1] The Union2 SNIa data are obtained, by adding new datapoints (including the high redshift SNIa) to the Union SNIa data, making a number of refinements to the Union analysis chain, refitting all light curves with the SALT2 fitter.

[2] The 397 Constitution data are obtained by adding 90 SNIa from CfA3 sample to 307 SNIa Union sample. CfA3 sample are all from the low-redshift SNIa, $z < 0.08$, and these 90 SNIa are calculated with using the same Union cuts.

combined constraint, we obtain the constraint results of MCG model parameters, $\Omega_k = -0.000844^{+0.013471}_{-0.015191}(1\sigma)^{+0.014536}_{-0.017862}(2\sigma)$, $B_s = 0.7541^{+0.0941}_{-0.0892}(1\sigma)^{+0.1092}_{-0.0965}(2\sigma)$, $\alpha = 0.0082^{+0.3837}_{-0.2318}(1\sigma)^{+0.4401}_{-0.2433}(2\sigma)$, $B = 0.00138^{+0.00817}_{-0.00738}(1\sigma)^{+0.00931}_{-0.00869}(2\sigma)$, with $\chi^2_{min} = 520.118(\chi^2_{min}/dof = 1.148)$. It seems that for this case, the MCG model tends to reduce to the flat cosmic concordance model, ΛCDM.

Acknowledgments The research work is supported by the National Natural Science Foundation (Grant No. 10875056), NSF (10703001), NSF (No.11005088) of P.R. China, and the Fundamental Research Funds for the Central Universities (DUT10LK31).

Appendix A: Current observational data and cosmological constraints

In this part we introduce the cosmological constraint methods and the current observed data used in this paper.

1. Type Ia supernovae

SNIa behave as the excellent standard candles, so they can be used to directly measure the expansion rate of the universe from the high redshift to the present time. For using SNIa data, theoretical dark-energy model parameters are determined by minimizing the quantity [70–77]

$$\chi^2_{SNIa}(\mu_0, p_s) = \sum_{i=1}^{N} \frac{(\mu_{obs}(z_i) - \mu_{th}(z_i; \mu_0, p_s))^2}{\sigma^2_{\mu_{obs}}(z_i)}, \tag{A1}$$

where $N = 557$ for Union2 dataset, which is the largest SNIa sample by far; p_s denotes the model parameters; $\sigma_{\mu_{obs}}(z_i)$ are errors; $\mu_{obs}(z_i) = m_{obs}(z_i) - M$, is the observed value of distance modulus of SNIa at z_i and can be given by the SNIa dataset; μ_{th} is the theoretical distance modulus, which is related to the apparent magnitude of SNIa at peak brightness m and the absolute magnitude M,

$$\mu_{th}(z) \equiv m_{th}(z) - M = 5\log_{10}(D_L(z)) + \mu_0. \tag{A2}$$

Here, the Hubble free luminosity distance

$$D_L(z) = H_0 d_L(z) = \frac{c(1+z)}{\sqrt{|\Omega_k|}} sinn\left[\sqrt{|\Omega_k|}\int_0^z \frac{H_0 dz'}{H(z'; p_s)}\right], \tag{A3}$$

and

$$\mu_0 = 5\log_{10}\left(\frac{H_0^{-1}}{Mpc}\right) + 25 = 42.38 - 5\log_{10} h, \tag{A4}$$

with h being a re-normalized quantity, which is given by $H_0 = 100h$ km s^{-1} Mpc^{-1}. It should be noted that μ_0 is independent of the data and the dataset. By expanding the χ^2 of Eq. (A1) relative to the nuisance parameter μ_0, the minimization with respect to μ_0 can be made trivially [78–80]

$$\chi^2_{SNIa}(p_s) = A(p_s) - 2\mu_0 B(p_s) + \mu_0^2 C, \tag{A5}$$

where

$$A(p_s) = \sum_{i=1}^{N} \frac{[\mu_{obs}(z_i) - \mu_{th}(z_i; \mu_0 = 0, p_s)]^2}{\sigma^2_{\mu_{obs}}(z_i)}, \tag{A6}$$

$$B(p_s) = \sum_{i=1}^{N} \frac{\mu_{obs}(z_i) - \mu_{th}(z_i; \mu_0 = 0, p_s)}{\sigma^2_{\mu_{obs}}(z_i)}, \tag{A7}$$

$$C = \sum_{i=1}^{N} \frac{1}{\sigma^2_{\mu_{obs}}(z_i)}. \tag{A8}$$

Obviously, according to Eq. (A5) χ^2_{SNIa} has a minimum for $\mu_0 = B/C$. Thus, the expression of χ^2 for SNIa constraint can be written as

$$\widetilde{\chi}^2_{SNIa}(p_s) = A(p_s) - B(p_s)^2/C. \tag{A9}$$

Since $\chi^2_{SNIa,min} = \widetilde{\chi}^2_{SNIa,min}$ and $\widetilde{\chi}^2_{SNIa}$ is independent of the nuisance parameter μ_0, one usually utilize the expression (A9) to displace (A1) to perform the likelihood analysis for the SNIa constraint. For minimizing $\chi^2_{SNIa}(p_s, B/C)$ to constrain cosmological model, it is equivalent to maximizing the likelihood

$$L(p_s) \propto \exp\left[\frac{-\chi^2(p_s)}{2}\right]. \tag{A10}$$

2. Observational Hubble data

The observational Hubble data [81,82] are based on differential ages of the galaxies. In [83], Jimenez et al. obtained an independent estimate for the Hubble parameter using the method developed in [84], and used it to constrain the cosmological models. The Hubble parameter depending on the differential ages as a function of redshift z can be written in the form of

$$H(z) = -\frac{1}{1+z}\frac{dz}{dt}. \tag{A11}$$

So, once dz/dt is known, $H(z)$ is obtained directly. By using the differential ages of passively-evolving galaxies from the Gemini Deep Deep Survey (GDDS) [85] and archival data [86–92], Simon et al. obtained several values of $H(z)$ at different redshift

Table 2 The observational $H(z)$ data [93–95]

z	0	0.1	0.17	0.27	0.4	0.48	0.88	0.9	1.30	1.43	1.53	1.75
$H(z)$ (km s^{-1} Mpc^{-1})	74.2	69	83	77	95	97	90	117	168	177	140	202
1σ uncertainty	±3.6	±12	±8	±14	±17	±60	±40	±23	±17	±18	±14	±40

[51]. The twelve observational Hubble data (redshift interval $0 \lesssim z \lesssim 1.8$) from Refs. [93–95] are listed in Table 2. In addition, in [96] the authors take the BAO scale as a standard ruler in the radial direction, and obtain three additional data: $H(z = 0.24) = 79.69 \pm 2.32$, $H(z = 0.34) = 83.8 \pm 2.96$, and $H(z = 0.43) = 86.45 \pm 3.27$.

The best fit values of the model parameters from observational Hubble data are determined by minimizing [97–100]

$$\chi^2_{OHD}(H_0, p_s) = \sum_{i=1}^{15} \frac{[H_{th}(H_0, p_s; z_i) - H_{obs}(z_i)]^2}{\sigma^2(z_i)}, \tag{A12}$$

where H_{th} is the predicted value of the Hubble parameter, H_{obs} is the observed value, $\sigma(z_i)$ is the standard deviation measurement uncertainty, and the summation is over the 15 observational Hubble data points at redshifts z_i.

3. The X-ray gas mass fraction

The X-ray gas mass fraction, f_{gas}, is defined as the ratio of the X-ray gas mass to the total mass of a cluster, which is approximately independent on the redshift for the hot ($kT \gtrsim 5$ keV), dynamically relaxed clusters at the radii larger than the innermost core r_{2500}. As inspected in [52], the ΛCDM model is very favored and has been chosen as the reference cosmology. The model fitted to the reference ΛCDM data is presented as [52]

$$f_{gas}^{\Lambda CDM}(z) = \frac{K A \gamma b(z)}{1 + s(z)} \left(\frac{\Omega_b}{\Omega_m}\right) \left[\frac{D_A^{\Lambda CDM}(z)}{D_A(z)}\right]^{1.5}, \tag{A13}$$

where $D_A^{\Lambda CDM}(z)$ and $D_A(z)$ denote respectively the proper angular diameter distance in the ΛCDM reference cosmology and the current constraint model. A is the angular correction factor, which is caused by the change in angle for the current test model θ_{2500} in comparison with that of the reference cosmology $\theta_{2500}^{\Lambda CDM}$:

$$A = \left(\frac{\theta_{2500}^{\Lambda CDM}}{\theta_{2500}}\right)^{\eta} \approx \left(\frac{H(z) D_A(z)}{[H(z) D_A(z)]^{\Lambda CDM}}\right)^{\eta}, \tag{A14}$$

here, the index η is the slope of the $f_{gas}(r/r_{2500})$ data within the radius r_{2500}, with the best-fit average value $\eta = 0.214 \pm 0.022$ [52]. And the proper (not comoving)

Table 3 The observational $r_s(z_d)/D_V(z)$ data [54]

z	$r_s(z_d)/D_V(z)$
0.2	0.1905 ± 0.0061
0.35	0.1097 ± 0.0036

angular diameter distance is given by

$$D_A(z) = \frac{c}{(1+z)\sqrt{|\Omega_k|}} sinn\left[\sqrt{|\Omega_k|}\int_0^z \frac{dz'}{H(z';\, p_s)}\right], \tag{A15}$$

which is related with $d_L(z)$ by

$$D_A(z) = \frac{d_L(z)}{(1+z)^2},$$

where $sinn(\sqrt{|\Omega_k|}x)$, respectively, denotes $\sin(\sqrt{|\Omega_k|}x)$, $\sqrt{|\Omega_k|}x$, $\sinh(\sqrt{|\Omega_k|}x)$ for $\Omega_k < 0$, $\Omega_k = 0$ and $\Omega_k > 0$.

In Eq. (A13), the parameter γ denotes permissible departures from the assumption of hydrostatic equilibrium, due to non-thermal pressure support; the bias factor $b(z) = b_0(1 + \alpha_b z)$ accounts for uncertainties in the cluster depletion factor; $s(z) = s_0(1 + \alpha_s z)$ accounts for uncertainties of the baryonic mass fraction in stars and a Gaussian prior for s_0 is employed, with $s_0 = (0.16 \pm 0.05)h_{70}^{0.5}$ [52]; the factor K is used to describe the combined effects of the residual uncertainties, such as the instrumental calibration and certain X-ray modelling issues, and a Gaussian prior for the 'calibration' factor is considered by $K = 1.0 \pm 0.1$ [52].

Following the method in Ref. [52,101] and adopting the updated 42 observational f_{gas} data in Ref. [52], the best fit values of the model parameters for the X-ray gas mass fraction analysis are determined by minimizing,

$$\chi^2_{CBF} = \sum_i^N \frac{[f_{gas}^{\Lambda CDM}(z_i) - f_{gas}(z_i)]^2}{\sigma^2_{f_{gas}}(z_i)} + \frac{(s_0 - 0.16)^2}{0.0016^2} + \frac{(K - 1.0)^2}{0.01^2} + \frac{(\eta - 0.214)^2}{0.022^2}, \tag{A16}$$

where $\sigma_{f_{gas}}(z_i)$ is the statistical uncertainties (Table 3 of [52]). As pointed out in [52], the acquiescent systematic uncertainties have been considered according to the parameters i.e. η, $b(z)$, $s(z)$ and K.

4. Baryon acoustic oscillation

The baryon acoustic oscillations are detected in the clustering of the combined 2dFGRS and SDSS main galaxy samples, which measure the distance–redshift relation at $z_{BAO} = 0.2$ and $z_{BAO} = 0.35$. The observed scale of the BAO calculated from

these samples, are analyzed using estimates of the correlated errors to constrain the form of the distance measure $D_V(z)$ [54,102,103]

$$D_V(z) = \left[(1+z)^2 D_A^2(z)\frac{cz}{H(z)}\right]^{1/3}. \tag{A17}$$

The peak positions of the BAO depend on the ratio of $D_V(z)$ to the sound horizon size at the drag epoch (where baryons were released from photons) z_d, which can be obtained by using a fitting formula [104]:

$$z_d = \frac{1291(\Omega_m h^2)^{-0.419}}{1+0.659(\Omega_m h^2)^{0.828}}[1+b_1(\Omega_b h^2)^{b_2}], \tag{A18}$$

with

$$b_1 = 0.313(\Omega_m h^2)^{-0.419}[1+0.607(\Omega_m h^2)^{0.674}], \tag{A19}$$
$$b_2 = 0.238(\Omega_m h^2)^{0.223}. \tag{A20}$$

In this paper, we use the data of $r_s(z_d)/D_V(z)$ extracted from the Sloan Digitial Sky Survey (SDSS) and the Two Degree Field Galaxy Redshift Survey (2dFGRS) [102,103], which are listed in Table 3, where $r_s(z)$ is the comoving sound horizon size

$$\begin{aligned} r_s(z) &= c\int_0^t \frac{c_s dt}{a} = c\int_0^a \frac{c_s da}{a^2 H} = c\int_z^\infty dz\frac{c_s}{H(z)} \\ &= \frac{c}{\sqrt{3}}\int_0^{1/(1+z)} \frac{da}{a^2 H(a)\sqrt{1+(3\Omega_b/(4\Omega_\gamma)a)}}, \end{aligned} \tag{A21}$$

where c_s is the sound speed of the photon−baryon fluid [105,106]:

$$c_s^{-2} = 3+\frac{4}{3}\times\frac{\rho_b(z)}{\rho_\gamma(z)} = 3+\frac{4}{3}\times\left(\frac{\Omega_b}{\Omega_\gamma}\right)a, \tag{A22}$$

and here $\Omega_\gamma = 2.469\times10^{-5}h^{-2}$ for $T_{CMB} = 2.725K$.

Using the data of BAO in Table 3 and the inverse covariance matrix V^{-1} in [54]:

$$V^{-1} = \begin{pmatrix} 30124.1 & -17226.9 \\ -17226.9 & 86976.6 \end{pmatrix}, \tag{A23}$$

the $\chi^2_{BAO}(p_s)$ is given as

$$\chi^2_{BAO}(p_s) = X^t V^{-1} X, \tag{A24}$$

where X is a column vector formed from the values of theory minus the corresponding observational data, with

$$X = \begin{pmatrix} \dfrac{r_s(z_d)}{D_V(0.2)} - 0.1905 \\ \dfrac{r_s(z_d)}{D_V(0.35)} - 0.1097 \end{pmatrix}, \tag{A25}$$

and X^t denotes its transpose.

5. Cosmic microwave background

The CMB shift parameter R is provided by [107]

$$R(z_*) = \sqrt{\Omega_m H_0^2}(1+z_*)D_A(z_*)/c, \tag{A26}$$

here, the redshift z_* (the decoupling epoch of photons) is obtained using the fitting function [108]

$$z_* = 1048\left[1 + 0.00124(\Omega_b h^2)^{-0.738}\right]\left[1 + g_1(\Omega_m h^2)^{g_2}\right],$$

where the functions g_1 and g_2 read

$$g_1 = 0.0783(\Omega_b h^2)^{-0.238}\left(1 + 39.5(\Omega_b h^2)^{0.763}\right)^{-1},$$
$$g_2 = 0.560\left(1 + 21.1(\Omega_b h^2)^{1.81}\right)^{-1}.$$

In addition, the acoustic scale is related to a distance ratio, $D_A(z)/r_s(z)$, and at decoupling epoch it is defined as

$$l_A \equiv (1+z_*)\frac{\pi D_A(z_*)}{r_s(z_*)}, \tag{A27}$$

where Eq. (A27) arises a factor $1+z_*$, because $D_A(z)$ is the proper (physical) angular diameter distance, whereas $r_s(z_*)$ is the comoving sound horizon. Using the data of l_A, R, z_* in [55] and their covariance matrix of $[l_A(z_*), R(z_*), z_*]$ (please see Tables 4 and 5), we can calculate the likelihood L as $\chi^2_{CMB} = -2\ln L$:

$$\chi^2_{CMB} = \triangle d_i [Cov^{-1}(d_i, d_j)[\triangle d_i]^t], \tag{A28}$$

where $\triangle d_i = d_i - d_i^{data}$ is a row vector, and $d_i = (l_A, R, z_*)$.

Table 4 The values of $l_A(z_*)$, $R(z_*)$, and z_* from 7-year WMAP data

	7-year maximum likelihood	error, σ
$l_A(z_*)$	302.09	0.76
$R(z_*)$	1.725	0.018
z_*	1091.3	0.91

Table 5 The inverse covariance matrix of $l_A(z_*)$, $R(z_*)$, and z_* from 7-year WMAP data

	$l_A(z_*)$	$R(z_*)$	z_*
$l_A(z_*)$	2.305	29.698	−1.333
$R(z_*)$		6825.270	−113.180
z_*			3.414

References

1. Riess, A.G., et al.: Astron. J. **116**, 1009 (1998). [arXiv:astro-ph/9805201]
2. Perlmutter, S., et al.: Astrophys. J. **517**, 565 (1999)
3. Spergel, D.N., et al.: Astrophys. J. Suppl. **148**, 175 (2003). [arXiv:astro-ph/0302209]
4. Pope, A.C., et al.: Astrophys. J. **607**, 655 (2004). [arXiv:astro-ph/0401249]
5. Weinberg, S.: Mod. Phys. Rev. **61**, 527 (1989)
6. Ratra, B., Peebels, P.J.E.: Phys. Rev. D. **37**, 3406 (1988)
7. Caldwell, R.R., Kamionkowski, M., Weinberg, N.N.: Phys. Rev. Lett. **91**, 071301 (2003). [arXiv:astro-ph/0302506]
8. Gong, Y.G., Wang, B., Cai, R.G.: JCAP **04**, 019 (2010). [arXiv:astro-ph/1001.0807]
9. Wu, P.X., Yu, H.W.: [arXiv:astro-ph/1007.2348]
10. Feng, B., Wang, X.L., Zhang, X.M.: Phys. Lett. B **607**, 35 (2005). [arXiv:astro-ph/0404224]
11. Xu, L.X., Lu, J.B., Li, W.B.: Eur. Phys. J. C. **64**, 89 (2009)
12. Lu, J.B., Saridakis, E.N., Setare, M.R., Xu. L.X.: JCAP, **03**, 031 (2010). [arXiv:astro-ph/0912.0923]
13. Li, M.: Phys. Lett. B **603**, 1 (2004). [arXiv:hep-th/0403127]
14. Gong, Y.G., Li, T.J.: Phys. Lett. B **683**, 241–247 (2010). [arXiv:astro-ph/0907.0860]
15. Wang, Y.T., Xu, L.X.: Phys. Rev. D **81**, 083523 (2010). [arXiv:1004.3340]
16. Kamenshchik, A.Y., Moschella, U., Pasquier, V.: Phys. Lett. B **511**, 265 (2001). [arXiv:gr-qc/0103004]
17. Makler, M., Oliveira, S.Q., Waga, I.: Phys. Lett. B **555**, 1 (2003)
18. Bean, R., Dore, O.: Phys. Rev. D **68**, 023515 (2003)
19. Dev, A., Jain, D., Alcaniz, J.S.: Astron. Astrophys. **417**, 847 (2004)
20. Amendola, L., Finelli, F., Burigana, C., Carturan, D.: JCAP **0307**, 005 (2003). [arXiv:astro-ph/0304325]
21. Jackiw, R.: [arXiv:physics/0010042]
22. Pedram, P., Jalalzadeh, S.: [arXiv:gr-qc/0711.1996]
23. Bento, M.C., Bertolami, O., Sen, A.: Phys. Rev. D **66**, 043507 (2002)
24. Bouhmadi-Lopez, M., Moniz, P.V.: Phys. Rev. D **71**, 063521 (2005)
25. Barrow, J.D.: Nucl. Phys. B **310**, 743–763
26. Benaoum, H.B.: [hep-th/0205140]
27. Sen, A.: [hep-th/0203211]
28. Sen, A.: [hep-th/0203256]
29. Padmanabhan, T.: [hep-th/0204150]
30. Paul, B.C., Thakur, P., Saha, A.: [arXiv:hep-th/0809.3491]
31. Paul, B.C., Thakur, P., Saha, A.: [arXiv:gr-qc/0707.4625]
32. Costa, S.S., Ujevic, M., Santos, A.F.: [arXiv:gr-qc/0703140]
33. Li, S., Ma, Y.G., Chen, Y.: Int. J. Mod. Phys. D **18**, 1785–1800 (2009)
34. Santos, F.C., Bedran, M.L., Soares, V.: Phys. Lett. B **646**, 215 (2007)
35. Bedran, M.L., Soares, V., Araujo, M.E.: Phys. Lett. B **659**, 462 (2008)
36. Barrow, J.D.: Phys. Lett. B **235**, 40 (1990)

37. Campo, S.D., Herrera, R.: [arXiv:astro-ph/0801.3251]
38. Herrera, R.: [arXiv:gr-qc/0805.1005]
39. Herrera, R.: [arXiv:gr-qc/0810.1074]
40. Jamil, M., Rashid, M.A.: [arXiv:astro-ph/0802.1146]
41. Jamil, M., Farooq, M.U., Rashid, M.A.: [arXiv:gr-qc/0901.2482]
42. Liu, D.J., Li, X.Z.: [arXiv:astro-ph/0501115]
43. Debnath, U., Banerjee, A., Chakraborty, S.: Class. Quant. Grav. **21**, 5609 (2004). [arXiv:gr-qc/0411015]
44. Feng, C.J., Li, X.Z.: [arXiv:astro-ph/0909.5476]
45. Chimento, L.P., Lazkoz, R.: [arXiv:astro-ph/0411068]
46. Chakraborty, W., Debnath, U.: [arXiv:gr-qc/0705.4147]
47. Debnath U., Chakraborty, S.: [arXiv:gr-qc/0601049]
48. Singha1 A.K., Debnath, U.: [arXiv:gr-qc/0701013]
49. Amanullah, R., et al.: [Supernova Cosmology Project Collaboration]. [arXiv:astro-ph/1004.1711]
50. The numerical data of the full sample are available at http://supernova.lbl.gov/Union
51. Simon, J., Verde, L., Jimenez, R.: Phys. Rev. D **71**, 123001 (2005). [arXiv:astro-ph/0412269]
52. Allen, S.W., Rapetti, D.A., Schmidt, R.W., Ebeling, H., Morris, R.G., Fabian, A.C.: Mon. Not. R. Astron. Soc. **383**, 879 (2008)
53. Eisenstein, D.J., et al.: Astrophys. J. **633**, 560 (2005). [arXiv:astro-ph/0501171]
54. Percival, W.J., et al.: [arXiv:astro-ph/0907.1660]
55. Komatsu, E., et al.: [arXiv:astro-ph/1001.4538]
56. Makler, M., Oliveira, S.Q., Waga, I.: Phys. Rev. D **68**, 123521 (2003)
57. Lima, J.A.S., Cunha, J.V., Alcaniz, J.S.: [arXiv:astro-ph/0611007]
58. Zhu, Z.H.: Astron. Astrophys. **423**, 421 (2004)
59. Wu, P.X., Yu, H.W.: Phys. Lett. B **644**, 16 (2007)
60. Silva, P.T., Bertolami, O.: Astrophys. J. **599**, 829–838 (2003). [arXiv:astro-ph/0303353]
61. Bento, M.C., Bertolami, O., Sen, A.A.: Phys. Lett. B **575**, 172–180 (2003). [arXiv:astro-ph/0303538]
62. Barreiro, T., Bertolami, O., Torres, P.: Phys. Rev. D **78**, 043530 (2008). [arXiv:0805.0731]
63. Lu, J.B., Gui, Y.X., Xu, L.X.: Eur. Phys. J. C. **63**, 349 (2009)
64. Chakraborty, S., Bandyopadhyay, T.: [arXiv:gr-qc/0707.1183]
65. Lewis, A., Bridle, S.: Phys. Rev. D **66**, 103511 (2002). http://cosmologist.info/cosmomc/
66. Rapetti, D., Allen, S.W., Weller, J.: Mon. Not. R. Astron. Soc. **360**, 555 (2005)
67. url:http://www.stanford.edu/drapetti/fgas-module/
68. Fabris, J.C., Ogouyandjou, C., Tossa, J., Velten, H.E.S.: [arXiv:astro-ph/1007.1011]
69. Hicken, M., et al.: Astrophys. J. **700**, 1097 (2009). [arXiv:astro-ph/0901.4804]
70. Guimaraes, A.C.C., Cunha, J.V., Lima, J.A.S.: JCAP **0910**, 010 (2009)
71. Lu, J.B.: Phys. Lett. B **680**, 404 (2009)
72. Szydlowski, M., Godlowski, W.: Phys. Lett. B **633**, 427 (2006). [arXiv:astro-ph/0509415]
73. Nesseris, S., Perivolaropoulos, L.: JCAP **0702**, 025 (2007). [arXiv:astro-ph/0612653]
74. Di Pietro, E., Claeskens, J.F.: Mon. Not. R. Astron. Soc. **341**, 1299 (2003). [arXiv:astro-ph/0207332]
75. Alam, U., Sahni, V.: Phys. Rev. D **73**, 084024 (2006)
76. Nesseris, S., Perivolaropoulos, L., J. Cosmol. Astropart. Phys. **0701**, 018 (2007). [arXiv:astro-ph/0610092]
77. Alam, U., Sahni, V., Saini, T.D., Starobinsky, A.A.: Mon. Not. R. Astron. Soc. **354**, 275 (2004)
78. Perivolaropoulos, L.: Phys. Rev. D **71**, 063503 (2005)
79. Nesseris, S., Perivolaropoulos, L.: Phys. Rev. D **72**, 123519 (2005). [astro-ph/0511040]
80. Li, M., Li, X.D., Wang, S., Zhang, X.: [arXiv:astro-ph/0904.0928]
81. Yi, Z.L., Zhang, T.J.: Mod. Phys. Lett. A **22**, 41–53 (2007). [arXiv:astro-ph/0605596]
82. Zhai, Z.X., Wan, H.Y., Zhang, T.J.: Physics Letters B **689**, 8–13, (2010). [arXiv:1004.2599]
83. Jimenez, R., Verde, L., Treu, T., Stern, D.: Astrophys. J. **593**, 622, (2003). [astro-ph/0302560]
84. Jimenez, R., Loeb, A.: Astrophys. J. **573**, 37 (2002). [arXiv:astro-ph/0106145].
85. Abraham, R.G., et al.: Astron. J. **127**, 2455 (2004). [arXiv:astro-ph/0402436]
86. Treu, T., Stiavelli, M., Casertano, S., Moller, P., Bertin, G.: Mon. Not. R. Astron. Soc. **308**, 1037 (1999)
87. Abraham, R.G., et al.: Astron. J. **593**, 622 (2003)
88. Treu, T., Stiavelli, M., Moller, P., Casertano, S., Bertin, G.: Mon. Not. Roy. Astron. Soc. **326**, 221 (2001). [astro-ph/0104177]
89. Treu, T., Stiavelli, M., Casertano, S., Moller, P., Bertin, G.: Astrophys. J. Lett. **564**, L13 (2002)

90. Dunlop, J., Peacock, J., Spinrad, H., Dey, A., Jimenez, R., Stern, D., Windhorst, R.: Nature **381**, 581 (1996)
91. Spinrad, H., Dey, A., Stern, D., Dunlop, J., Peacock, J., Jimenez, R., Windhorst, R.: Astrophys. J. **484**, 581 (1997)
92. Nolan, L.A., Dunlop, J.S., Jimenez, R., Heavens, A.F.: Mon. Not. R. Astron. Soc. **341**, 464 (2003); [astro-ph/0103450]
93. Stern, D., Jimenez, R., Verde, L., Kamionkowski, M., Stanford, S.A.: [arXiv:astro-ph/0907.3149]
94. Simon, J., et al.: Phys. Rev. D **71**, 123001 (2005)
95. Riess, A.G., et al.: [arXiv:0905.0695]
96. Gaztanñaga, E., Cabré, A., Hui, L.: [arXiv:0807.3551]
97. Lazkoz, R., Majerotto, E.: JCAP **0707**, 015 (2007). [arXiv:astro-ph/0704.2606]
98. Lu, J.B., Xu, L.X., Liu, M.L., Gui, Y.X: Eur. Phys. J. C **58**, 311 (2008). [arXiv:astro-ph/0812.3209]
99. Samushia, L., Ratra, B.: Astrophys. J. **650**, L5 (2006). [astro-ph/0607301]
100. Jimenez, R., Verde, L., Treu, T., Stern, D.: Astrophys. J. **593**, 622 (2003). [astro-ph/0302560]
101. Nesseris S., Perivolaropoulos, L.: JCAP **0701**, 018 (2007). [astro-ph/0610092]
102. Eisenstein, D.J., et al.: Astrophys. J. **633**, 560 (2005)
103. Percival, W.J., et al.: Mon. Not. R. Astron. Soc. **381**, 1053 (2007)
104. Eisenstein, D.J., Hu, W.: Astrophys. J. **496**, 605 (1998). [arXiv:astro-ph/9709112]
105. Hu, W., Sugiyama, N.: Astrophys. J. **444**, 489 (1995). [arXiv:astro-ph/9407093]
106. Hu, W., Fukugita, M., Zaldarriaga, M., Tegmark, M.: Astrophys. J. **549**, 669 (2001). [arXiv:astro-ph/0006436]
107. Bond, J.R., Efstathiou, G., Tegmark, M.: Mon. Not. R. Astron. Soc. **291**, L33 (1997)
108. Hu, W., Sugiyama, N.: Astrophys. J. **471**, 542 (1996)